First-principles dynamical calculation of a pump-probe scenario for the spin flip on NiO: Dynamical vs static calculation of the susceptibility tensor

Georgios Lefkidis* and Wolfgang Hübner

Department of Physics and Research Center OPTIMAS, University of Kaiserslautern, PO Box 3049, 67653 Kaiserslautern, Germany

(Received 24 July 2012; revised manuscript received 16 January 2013; published 28 January 2013)

Using a fully *ab initio* approach we calculate in a dynamic way the susceptibility through the time-dependent probe signal of a spin-flip scenario on the antiferromagnetic NiO (001) surface using linear-response theory. To this end we obtain the highly correlated wave function of the system and we propagate it under the influence of both a pump and a probe pulse of the same frequency, a situation usually encountered in experiment. Thus we treat both pulses on equal footing and, for the first time, consider the effects of the electronic nonequilibrium on the susceptibility due to the *concurrent* presence of the pulses. Our time-resolved calculations reveal the subtle influence of the probe pulse itself on the detection signal, which cannot be completely accounted for solely by the time propagation of the pump pulse and the subsequent static calculation of the susceptibility tensor. We calculate the dynamical Stark effect, a broadening of the peaks, optical interference effects, and satellite peaks.

DOI: 10.1103/PhysRevB.87.014432 PACS number(s): 75.78.Jp, 78.20.Bh, 78.47.J−, 78.20.Ls

I. INTRODUCTION

Immediately following the eve of laser-induced spin manipulation in magnetically ordered materials,[1] a huge amount of relevant theoretical and experimental work has been performed in order to determine the exact microscopic mechanisms of the induced spin behavior.[2–4] One of the main challenges is to investigate the precise nature and the possible effects of the experimental setup as opposed to the theoretical models, and thus establish a common language among experimentalists and theorists. Although the ongoing debate with respect to the driving microscopic mechanisms seems to slowly converge to the conclusion that at least at short times the photon-electron interaction plays the major role,[2,5–9] the question of what is actually being measured in the experiment still remains.[10] Recent experiments show that the helicity of the light plays a major role in all-optical magnetic switching, and a theoretical study on subpicosecond spin dynamics in hydrogenlike systems indicates that the stimulated Raman scattering process leads to a change of the magnetic state of the system.[11,12] A typical situation occurs in pump-probe experiments: While usually it is a theorist's intention to concentrate on the pump pulse, an experimentalist's need to include the probe pulse for measuring purposes can potentially influence the outcome of the detection setup. The potential of a second (probe) pulse to alter the polarization and the spin moment was recently investigated.[13] Here we address this very interesting topic and go even further: We compute the experimentally relevant susceptibility tensor by calculating the polarization induced in the system for several combinations of pump and probe pulses, with respect to their amplitudes, time separation, and relative phase. This way we are able to calculate the dynamical Stark effect, a broadening of the peaks, and satellite peaks as well as optical interference effects due to the probe pulse.

This manuscript is organized as follows. In Sec. II the system and the methods are presented, and in Sec. III the details of the static and the dynamical calculation of the susceptibility tensor are presented. The results are further discussed in Sec. IV, and finally some conclusions are drawn (Sec. V).

II. SYSTEM AND METHODS

We calculate the lowest energy states of a doubly embedded NiO_5^{-8} cluster (point group C_{4v}), first in a layer of effective core potentials which account for the Ni atoms in the immediate vicinity and then in a $15 \times 15 \times 8$ grid of point charges which describes the Madelung potential. All 45 intragap d states are obtained with the complete-active-space self-consistent-field (CAS-SCF) method and compare very well with experiment.[14–16] CAS-SCF is most suitable for static correlations,[17–21] the importance of which in laser-induced spin-switching processes has already been established.[22] Methods based on density functional theory (DFT) like time-dependent DFT compare favorably with configuration-interaction singles calculations (fewer correlations than CAS-SCF) and work within the linear-response regime.[23] Although the pump pulse is sufficiently weak to guarantee the validity of time-dependent perturbation theory (numerically ascertained by the conservation of the total population) it is strong enough to induce appreciable magnetic effects (spin flip). Thus, as will be shown below, a particular strength of our theoretical framework is to yield pump-induced effects well beyond the linear-response regime. We correlate all 10 d-character molecular orbitals and include up to 24 configurations using the Los Alamos basis set.[24,25] Then spin-orbit coupling (SOC) and an infinitesimal static magnetic field are included perturbatively. SOC splits the lowest intragap terms ($1^3B_1 \rightarrow 1B_2 + 1E$, $1^3E \rightarrow 1A_1 + 1A_2 + 2E + 1B_1 + 2B_2$, $1^3B_2 \rightarrow 2B_1 + 3E$ with energy splittings 3.2, 142.3, and 18 meV, respectively) and thus facilitates the $d \leftrightarrow d$ transitions.[18]

Finally a laser pulse with a sech^2-shaped envelope and frequency $\omega_{\mathrm{laser}} = 0.443$ eV is applied by means of time-dependent perturbation theory within the interaction picture:[26]

$$\frac{\partial c_n}{\partial t} = -\frac{i}{\hbar}\sum_k \langle n|\hat{H}'|k\rangle c_k(t) e^{-i(E_k - E_n)t/\hbar}, \qquad (1)$$

where $|n\rangle$ and $|k\rangle$ are the unperturbed eigenstates, c_n is the complex scalar coefficient of state $|k\rangle$ in the total wave function $\psi(t) = \sum_n c_n(t) e^{-iE_n t/\hbar}|n\rangle$, and E_n is the energy of state $|n\rangle$. $\hat{H}' = \hat{\mathbf{d}} \cdot \mathbf{E}(t)$ is the perturbation term in the Hamiltonian, $\mathbf{E}(t)$

is the electric field of the pulse (its maximum value at the peak of the pulse is $E_{\max} = 5 \times 10^{10}$ V/m), and $\hat{\mathbf{d}}$ is the electric-dipole operator. We propagate all 45 states with an embedded fifth-order Runge-Kutta method and the Cash-Karp adaptive step control.[27] The typical time step is 25 attoseconds.

The laser pulse flips the direction of the spin expectation value from pointing downward to upward. To this end it transfers the population from the spin-down to the spin-up state through one or more intermediate, spin-mixed, optically addressable excited states ($|\downarrow\downarrow\rangle \rightarrow |e\rangle \rightarrow |\uparrow\uparrow\rangle$). In analogy to three-level model systems we call this a Λ process.[28,29] In previous works we calculated the time-dependent induced polarization $\mathbf{P}(t)$ in the material and by Fourier transforming it using a window function we showed that the material selectively absorbs or emits light of the necessary helicity, provided that the latter is present.[30,31] Specifically we showed that the cluster absorbs right-handed circularly polarized light σ_+ during the absorption phase ($|\downarrow\downarrow\rangle \rightarrow |e\rangle$) and emits left-handed circularly polarized light σ_- during the emission phase ($|e\rangle \rightarrow |\uparrow\uparrow\rangle$). Therefore the spin-flipping light needs to be of linear polarization (or at least to contain both σ_+ and σ_- components).

In the above-mentioned work we did not delve into how the induced material polarization is detected in a pump-probe experiment. In experiment the relevant quantity is the susceptibility tensor χ and what is actually being measured is the intensity of the reflected (or transmitted) light as a function of the incident probe pulse. Since χ depends on the electronic structure of the material, driving the latter away from equilibrium alters χ as well. However, it is not only the repopulation of the states but also quantum interferences that affect χ. These interferences do far more than changing the intensity of the observed peaks; they can also shift them and create new satellite peaks, effects that cannot be attributed to population changes alone.

III. SUSCEPTIBILITY TENSOR

In order to investigate and discriminate the effects of the quantum interferences we take two steps. As a first step we restrict our study to the direct time-dependent influence of the pump pulse and calculate the first-order susceptibility tensor *statically*[32] as

$$\chi^{(1)}(\omega) \propto \sum_{a,b} D^*_{ab} D_{ba} \frac{n_a - n_b}{E_a - E_b - \hbar\omega + i\hbar\Gamma}, \qquad (2)$$

where D_{ab} are the dipole-transition-matrix elements between states $|a\rangle$ and $|b\rangle$, n_a and n_b are the populations of the states, E_a and E_b are their energies, ω is the frequency of the probing pulse, and Γ is a broadening constant, which with our quantum chemical method cannot be calculated and is therefore set equal to an empirical value of 0.05 eV. Equation (2) suggests that only the intensity of the peaks can change through repopulation and not their energetic position, since the energies in the denominator remain constant. These peaks can obviously occur only at resonances between the unperturbed (by the light) states. We calculate $\chi^{(1)}(\omega)$ both for right [$D^{(+)}_{ab} = D^{(x)}_{ab} + i\,D^{(y)}_{ab}$] and left [$D^{(-)}_{ab} = D^{(x)}_{ab} - i\,D^{(y)}_{ab}$] circular polarizations, which correspond to positive and negative, respectively, helicities of a probe pulse (Fig. 1). The energy positions in both cases coincide exactly with energy differences between the initial and the intermediate states (for σ_+ during the absorption phase), and between the intermediate states and the final state (for σ_- during the emission phase). Since the initial and the final states are quasidegenerate (only Zeeman splitting of about 1 meV) the positions are almost identical. From the number of the peaks one might erroneously deduce that only two excited states function as intermediate states. Inspection of the time-dependent populations, however, reveals that 12 states attain at some point populations larger than 0.001.[26] In fact recent results show that some excited states may play a crucial role while still remaining essentially unpopulated throughout such processes [e.g., see Fig. 2(c) in Ref. 33]. Conceptually this way of calculating the susceptibility tensor is similar to treating the nonlinear response as a pure Kerr effect,[34] which is not valid for ultrafast laser pulses where the instantaneous Kerr model breaks down.[35]

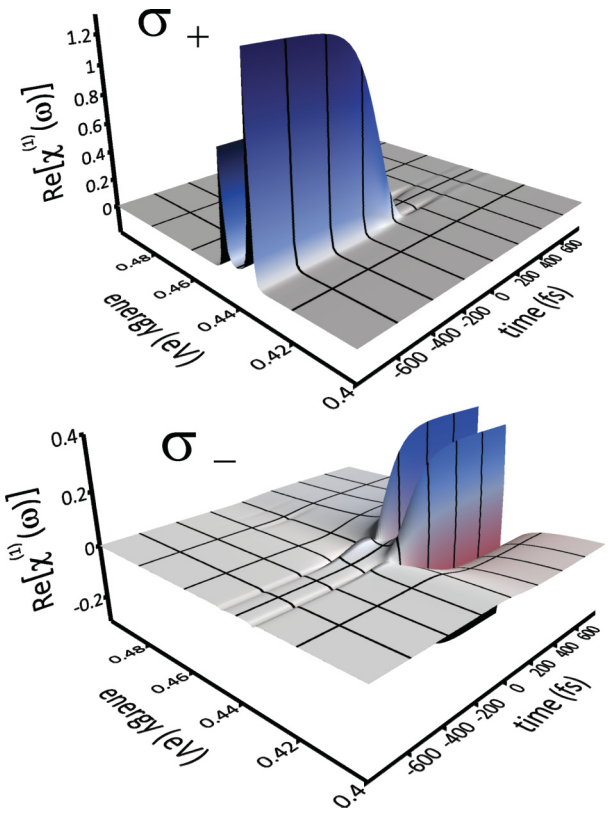

FIG. 1. (Color online) Time-dependent susceptibility tensor $\chi^{(1)}(\omega)$, calculated *statically* with Eq. (2) for different times during the irradiation of the cluster with the pump pulse (in arbitrary units). The upper panel depicts the first-order susceptibility for positive (σ_+) and the lower panel for negative (σ_-) probe-pulse helicity.

In a second step, which we call *dynamical*, we irradiate the cluster with *both* the pump and the probe pulses and again propagate in time for different probe delays τ (the pump laser parameters are kept the same, the probe pulse has the same frequency and propagation direction as the pump pulse, but either right or left helicity and 5% of the amplitude of the pump). We define the susceptibility tensor as $\chi(\omega) = \frac{\partial \mathbf{P}(\omega)}{\partial \mathbf{E}_{\text{probe}}(\omega)}$, where $\mathbf{P}(\omega)$ is the induced polarization in the material and $\mathbf{E}_{\text{probe}}(\omega)$ is the electric field of the probing

laser pulse, therefore for every time step we need to propagate several times with slightly different probe-pulse amplitudes in order to calculate the derivative (we use Simpson's 3/8 rule). Note that $\mathbf{P}$ depends on both the pump and the probe pulses and thus includes all wave-mixing combinations as well. Since the measurement gives a time-dependent signal at a fixed frequency we define the time-windowed susceptibility tensor in the frequency domain $\tilde{\chi}(\omega,t)$ as obtained by Fourier-transforming $\mathbf{P}(t)$ and $\mathbf{E}_{\text{probe}}(t)$ with a window function G [for computational convenience the vacuum permittivity ε_0 is absorbed in $\tilde{\chi}(\omega,t)$]:

$$\tilde{\chi}(\omega,t) = \left.\frac{\int \mathbf{P}(t')G(\sigma,t-t')e^{i\omega t'}\,dt'}{\int \mathbf{E}_{\text{probe}}(t')G(\sigma,t-t')e^{i\omega t'}\,dt'}\right|_{\omega_{\text{laser}}}, \qquad (3)$$

where $G(\sigma,t-t')$ is the normalized Gaussian distribution centered at t with standard deviation σ [note that the numerator in Eq. (3) is nothing more than Eq. (1) of Ref. 30]. In practice we investigate the frequency area around ω_{laser} for $\mathbf{P}(\omega)$. This is exactly why $\tilde{\chi}(\omega,t)$ has no peaks at distant energies: There is no probe pulse to query them. This might appear as a drawback as compared to the statically calculated tensor, but it better reflects the real situation. The frequency for both pulses is set equal to the frequency of the spin-flipping pump pulse $\omega_{\text{laser}} = 0.443$ eV.

IV. DISCUSSION

Compared to the static case the dynamical calculation has one important additional aspect: Since the pump and the probe pulses partially overlap they can interfere constructively (Fig. 2), destructively, or even in an alternating manner (Fig. 3). This is decided by the way the experiment is carried out (with or without phase locking).[36] If both pulses originate from the same source and the probe pulse is simply delayed by means of a longer path, then the third case happens and a beating with the optical frequency occurs:[37]

$$\mathbf{E}_{\text{probe}}(t) = aA_{\text{pump}}(t-\tau)\mathbf{E}^{(0)}_{\text{pump}}\cos(\omega_{\text{laser}}t-\phi) \qquad (4)$$

where $\mathbf{E}^{(0)}_{\text{pump}}$ is the amplitude of the pump pulse, $A_{\text{pump}}(t)$ its envelope function, a is the ratio of the maximum amplitudes of the probe and the pump pulses (5% in our case), and $\phi = \omega_{\text{laser}}\tau$ the phase difference between pump and probe. Clearly ϕ depends on τ, unless the probe pulse is phase-modulated (which, in two extreme cases, leads to completely constructive or destructive interferences). In our calculations we see no quantum interferences after the pump pulse since we expand the wave function in many-body states which are already eigenstates of the Hamiltonian (i.e., they include correlations). One should bear in mind that our genetic algorithm explicitly aims at populating only a pure final state in this basis. One might argue that over a period this averages out (rotating-wave-like approximation), but (i) this remains an approximation, if legitimate, and (ii) it does not reveal the underlying differences between different interference patterns [compare Figs. 2 (upper panel) and 3]. The dynamical calculation of $\tilde{\chi}$ conceptually includes terms linear in the weak $\mathbf{E}_{\text{probe}}$ field but of all orders in the $\mathbf{E}_{\text{pump}}$ field, hence we do not need to distinguish between orders $\chi^{(1)}$, $\chi^{(2)}$, $\chi^{(3)}$, etc. Figure 2 shows the fourth component of the Stokes vector

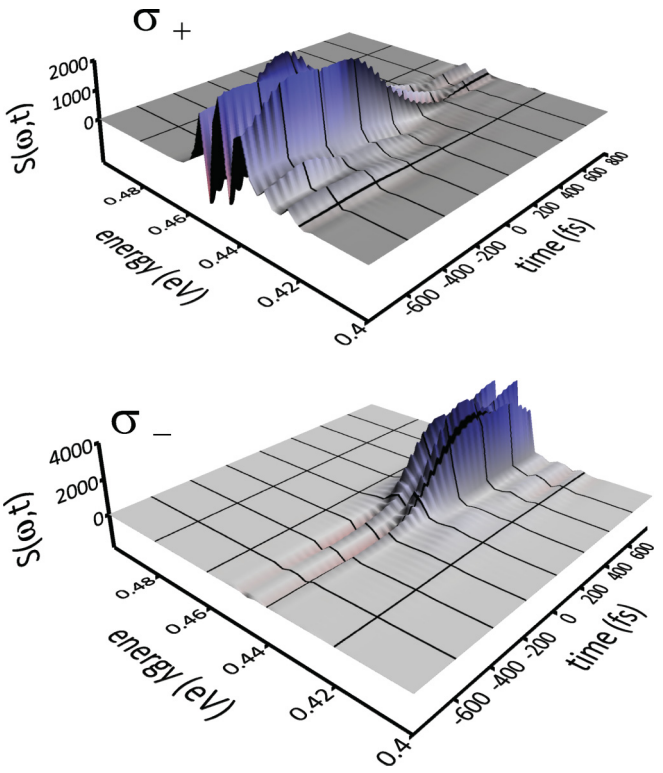

FIG. 2. (Color online) Fourth component of the Stokes vector derived from the time-dependent susceptibility tensor $\chi(\omega)$, calculated dynamically for phase-locked, constructive interference of pump and probe pulses (in arbitrary units). The upper panel depicts the susceptibility for positive (σ_+) and the lower panel for negative (σ_-) probe-pulse helicity.

$S = 2\text{Im}(\chi_{x,\sigma_+}\chi^*_{y,\sigma_+})$ for the first case (constructive interference) and Fig. 3 for the last case (alternating phase difference). In the tensor element χ_{i,σ_j}, σ_j refers to the polarization of the laser pulse and i to the induced polarization in the material.

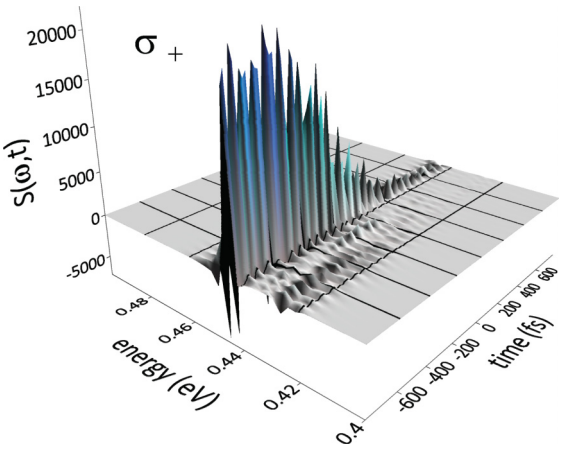

FIG. 3. (Color online) Fourth component of the Stokes vector derived from the time-dependent susceptibility tensor $\chi(\omega)$ in arbitrary units, calculated dynamically for pump and probe pulses having alternating phase difference $\phi = \omega\tau$ (longer path for the probe pulse and no-phase locking, see text). The probe pulse has σ_+ helicity (absorption phase). The beatings are clearly visible (the calculations are performed with 1 fs pump-probe time-delay steps).

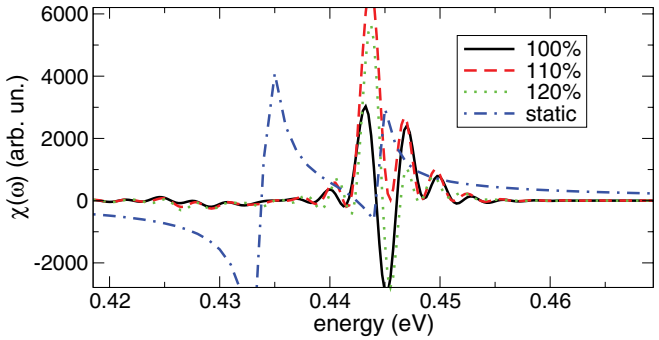

FIG. 4. (Color online) Dynamical calculation of the susceptibility tensor χ for a pump-probe delay of 100 fs and σ_+ helicity of the probe pulse (for the in-phase case, see discussion in text and Fig. 2). There are several satellite peaks not present in the static calculation. The black, solid line is for the optimized pump laser pulse. The red dashed line and the green dotted line are for a 10% and 20% increase in the pump's amplitude, respectively. Note the blue-shift of the main peak at 0.443 of about 6 meV, when the pump's amplitude is increased. The blue dash-dotted line is the susceptibility tensor from the static calculation (see Fig. 1).

Compared to the static calculation (Fig. 1) one notices the following differences: (i) the dynamic calculation reveals a richer spectrum throughout the whole process. Some satellite peaks appear at frequencies which do not correspond to energy differences of electronic levels (check the peak at 0.45 eV and the splitting of the dominant peak at 0.445 eV in Fig. 4), (ii) there is some broadening (which unlike the static case comes out of the calculation directly—there is no empirical parameter Γ here), (iii) some shifting of the peaks takes place (dynamical Stark effect), more specifically the central peaks get red-shifted during absorption and blue-shifted during emission (about 3 meV when the amplitude of the pump pulse increases by 10%, see Fig. 4), and (iv) the maximum of the satellite peaks (unlike the others) is not attained at infinite times before or after the process (like all peaks in the static calculation), but on the onset and the end of it, for right and left probe helicities, respectively (Fig. 2). These differences can be mainly attributed to three effects: (i) in the dynamic calculation we implicitly include more photon processes (pump and probe pulses), (ii) the probe pulse also affects the electronic transfer during the process, thus slightly altering the population of the states at any given time (compare to two simple Rabi oscillations with slightly different laser amplitudes—at the same time the populations differ), and (iii) we explicitly take into account the phase differences between pump and probe pulses which lead to interference effects along the frequency axis (therefore the satellite peaks can get slightly shifted). Keep in mind that although the response of the system is linear in the probe pulse [implied in the definitions of both $\chi^{(1)}(\omega)$ and $\tilde{\chi}(\omega,t)$], this is not the case for the pump pulse (changing it practically induces a different Λ process).

V. CONCLUSIONS

In summary we calculate and compare the time-dependent susceptibility tensor for an ultrafast, spin-flipping, laser-driven Λ process in two different ways, i.e., statically and dynamically. We find that the usual static calculation allows us to draw conclusions about the helicity of the detected light, in the same manner that the calculation of the induced material polarization does, and shows that the material absorbs and emits the appropriate helicities. There are, however, important effects which cannot be calculated in this way, and necessitate the concurrent propagation of both the pump and the probe pulses in time. These effects are (i) the dynamical Stark effect, (ii) the existence of satellite peaks, which attain their maximum on the onset or near the end of the process, (iii) the existence of optical interference effects between the pump and the probe pulses, and (iv) broadening of the peaks. In a whole, we present a method of calculating the outcome of an optical experiment which takes into account the probe pulse, and thus gives insight into the perturbative nature of the measurement itself for complex correlated systems.

ACKNOWLEDGMENTS

We would like to acknowledge financial support from the German Research Foundation (DFG) through an Individual Grant and the Transregional Collaborative Research Center SFB/TRR88 "3MET."

*lefkidis@physik.uni-kl.de

[1]E. Beaurepaire, J.-C. Merle, A. Daunois, and J.-Y. Bigot, Phys. Rev. Lett. **76**, 4250 (1996).
[2]J.-Y. Bigot, M. Vomir, and E. Beaurepaire, Nat. Phys. **5**, 515 (2009).
[3]B. Koopmans, J. J. M. Ruigrok, F. Dalla Longa, and W. J. M. de Jonge, Phys. Rev. Lett. **95**, 267207 (2005).
[4]A. V. Kimel, A. Kirilyuk, P. A. Usachev, R. V. Pisarev, A. M. Balashov, and T. Rasing, Nature (London) **435**, 6558 (2005).
[5]H. Vonesch and J.-Y. Bigot, Phys. Rev. B **85**, 180407(R) (2012).
[6]L. Cywinski and L. J. Sham, Phys. Rev. B **76**, 045205 (2007).
[7]I. Radu, G. Woltersdorf, M. Kiessling, A. Melnikov, U. Bovensiepen, J.-U. Thiele, and C. H. Back, Phys. Rev. Lett. **102**, 117201 (2009).
[8]E. Šimánek and B. Heinrich, Phys. Rev. B **67**, 144418 (2003).
[9]D. Meier, M. Maringer, T. Lottermoser, P. Becker, L. Bohatý, and M. Fiebig, Phys. Rev. Lett. **102**, 107202 (2009).
[10]H.-S. Rhie, H. A. Dürr, and W. Eberhardt, Phys. Rev. Lett. **90**, 247201 (2003).
[11]D. Popova, A. Bringer, and S. Blügel, Phys. Rev. B **85**, 094419 (2012).
[12]J. A. de Jong, I. Razdolski, A. M. Kalashnikova, R. V. Pisarev, A. M. Balbashov, A. Kirilyuk, T. Rasing, and A. V. Kimel, Phys. Rev. Lett. **108**, 157601 (2012).
[13]G. P. Zhang, Phys. Rev. B **85**, 224407 (2012).
[14]A. Gorschlüter and H. Merz, Phys. Rev. B **49**, 17293 (1994).
[15]M. Fiebig, D. Fröhlich, T. Lottermoser, V. V. Pavlov, R. V. Pisarev, and H.-J. Weber, Phys. Rev. Lett. **87**, 137202 (2001).

[16]A. Rubano, T. Satoh, A. Kimel, A. Kirilyuk, T. Rasing, and M. Fiebig, Phys. Rev. B **82**, 174431 (2010).
[17]M. Geleijns, C. de Graaf, R. Broer, and W. Nieuwpoort, Surf. Sci. **421**, 106 (1999).
[18]K. Satitkovitchai, Y. Pavlyukh, and W. Hübner, Phys. Rev. B **72**, 045116 (2005).
[19]G. Lefkidis and W. Hübner, Phys. Rev. Lett. **95**, 077401 (2005).
[20]M. van Veenendaal, X. Liu, M. H. Carpenter, and S. P. Cramer, Phys. Rev. B **83**, 045101 (2011).
[21]B. Fromme, M. Möller, T. Anschütz, C. Bethke, and E. Kisker, Phys. Rev. Lett. **77**, 1548 (1996).
[22]G. P. Zhang, G. Lefkidis, W. Hübner, and Y. Bai, J. Appl. Phys. **109**, 07D303 (2011).
[23]M. Petersilka, U. J. Gossmann, and E. K. U. Gross, Phys. Rev. Lett. **76**, 1212 (1996).
[24]W. R. Wadt and P. J. Hay, J. Chem. Phys. **82**, 284 (1985).
[25]M. J. Frisch *et al.*, "*Gaussian 03, Revision B.03*" (Gaussian, Inc., Wallingford, CT, 2004).
[26]G. Lefkidis and W. Hübner, Phys. Rev. B **76**, 014418 (2007).
[27]R. R. Cash and A. H. Karp, ACM Trans. Math. Software **16**, 201 (1990).
[28]L. Slodička, G. Hétet, S. Gerber, M. Hennrich, and R. Blatt, Phys. Rev. Lett. **105**, 153604 (2010).
[29]B. W. Shore, K. Bergmann, J. Oreg, and S. Rosenwaks, Phys. Rev. A **44**, 7442 (1991).
[30]G. Lefkidis, G. P. Zhang, and W. Hübner, Phys. Rev. Lett. **103**, 217401 (2009).
[31]G. Lefkidis and W. Hübner, Phys. Rev. B **87**, 014404 (2013).
[32]W. Hübner and K.-H. Bennemann, Phys. Rev. B **40**, 5973 (1989).
[33]C. Li, W. Jin, H. P. Xiang, G. Lefkidis, and W. Hübner, Phys. Rev. B **84**, 054415 (2011).
[34]R. S. Beni, Y.-K. Yoon, R. W. Boyd, and J. E. Sipe, Opt. Lett. **24**, 1416 (1999).
[35]M. Conforti and G. Della Valle, Phys. Rev. B **85**, 245423 (2012).
[36]N. F. Scherer, A. J. Ruggiero, M. Du, and G. R. Fleming, J. Chem. Phys. **93**, 856 (1990).
[37]V. Blanchet, C. Nicole, M.-A. Bouchene, and B. Girard, Phys. Rev. Lett. **78**, 2716 (1997).